476 *Inorg. Chem.* **2010**, *49*, 476–487
DOI: 10.1021/ic9016323

Inorganic Chemistry
Article

Luminescent Platinum Complexes with Terdentate Ligands Forming 6-Membered Chelate Rings: Advantageous and Deleterious Effects in N^N^N and N^C^N-Coordinated Complexes

Katherine L. Garner, Louise F. Parkes, Jason D. Piper, and J. A. Gareth Williams*

Department of Chemistry, University of Durham, Durham DH1 3LE, U.K.

Received August 14, 2009

Platinum(II) complexes of the form $[PtL^nCl]^+$ are reported, containing the N^N^N-coordinating ligands 2,6-di-(8-quinolyl)pyridine (L^1), 2,6-di(8-quinolyl)-4-methoxypyridine (L^2), or 2,6-di(7-aza-indolyl)-pyridine (L^3). Metathesis of the chloride co-ligand in $[PtL^1Cl]^+$ can be accomplished under mild conditions, as exemplified by the formation of the complexes $[PtL^1OMe]^+$ and $[PtL^1(C{\equiv}C\text{-tfp})]^+$, in which L^1 remains bound as a terdentate ligand {HC≡C-tfp = 3,5-bis(trifluoromethyl)-phenylacetylene}. An N^C^N-coordinated, cyclometalated analogue of $[PtL^1Cl]^+$ has also been prepared, namely, PtL^4Cl where HL^4 is 1,3-di(8-quinolyl)benzene. The common feature among the six new complexes described here is that they contain 6-membered chelate rings, rather than the usual 5-membered rings that form when more common N^N^N ligands, such as 2,2′:6′,2″-terpyridine (tpy), bind to Pt(II). All the quinolyl-based complexes are phosphorescent in solution at room temperature, with quantum yields up to 4%. This contrasts with the well-established lack of emission from $[Pt(tpy)Cl]^+$ under these conditions. Density functional theory calculations suggest that the improvement may stem, at least in part, from the relief of ring strain associated with the larger chelate ring size, leading to a more optimal bite angle at the metal, close to 180°, and hence to a stronger ligand field. Consideration of the luminescence parameters, including data at 77 K, together with absorption and electrochemical data and the results of TD-DFT calculations, suggests that the lowest-lying singlet states have metal-to-ligand charge-transfer (MLCT) character, but that the triplet state from which emission occurs has more predominant ligand-centered character. The azaindolyl complex $[PtL^3Cl]^+$ is not emissive at room temperature, apparently owing to a particularly small radiative rate constant. The cyclometalated complex PtL^4Cl emits at lower energy than $[PtL^1Cl]^+$ but, in this case, the luminescence quantum yield is inferior to related complexes with 5-membered chelate rings.

Introduction

Research into the design and preparation of photoluminescent platinum(II) complexes has been driven by a number of applications such as triplet-harvesting phosphors for light-emitting devices,[1] chemosensing,[2] chromophores for promoting photoinduced charge separation for artificial photosynthesis,[3] probes for biological molecules such as nucleic acids and proteins,[4] and bioimaging agents.[5] At the more fundamental level too, studies on emissive platinum complexes have provided insight into key excited state processes such as intersystem crossing[6] and spin−orbit coupling pathways.[7]

A clear picture has emerged over the past 20 years of the molecular features that are likely to favor triplet emission over non-radiative decay in square-planar Pt(II) complexes.

*To whom correspondence should be addressed. E-mail: j.a.g.williams@durham.ac.uk.

(1) (a) Xiang, H.-F.; Lai, S.-W.; Lai, P. T.; Che, C.-M. Phosphorescent platinum(II) materials for OLED applications. In *Highly efficient OLEDs with phosphorescent materials*; Yersin, H., Ed.; Wiley-VCH: Weinheim, 2008. (b) Williams, J. A. G.; Develay, S.; Rochester, D. L.; Murphy, L. *Coord. Chem. Rev*. **2008**, *252*, 2596.

(2) (a) Fletcher, N.; Lagunas, M. C. *Top. Organomet. Chem*. **2010**, *28*, 143. (b) Tang, W.-S.; Lu, X.-X.; Wong, K.M.-C.; Yam, V.W.-W. *J. Mater. Chem*. **2005**, *15*, 2714. (c) Siu, P. K. M.; Lai, S.-W.; Lu, W.; Zhu, N.; Che, C.-M. *Eur. J. Inorg. Chem*. **2003**, 2749. (d) Yang, Q.-Z.; Tong, Q.-X.; Wu, L.-Z.; Zhang, L.-P.; Tung, C.-H. *Eur. J. Inorg. Chem*. **2004**, 1948. (e) Lanoë, P.-H.; Fillaut, J.-L.; Toupet, L.; Williams, J. A. G.; Le Bozec, H.; Guerchais, V. *Chem. Commun*. **2008**, 4333.

(3) Chakraborty, S.; Wadas, T. J.; Hester, H.; Schmehl, R.; Eisenberg, R. *Inorg. Chem*. **2005**, *44*, 6865.

(4) (a) Eryazici, I.; Moorefield, C. N.; Newkome, G. R. *Chem. Rev*. **2008**, *108*, 1834. (b) Wong, K.M.-C.; Tang, W. S.; Chu, B. W. K.; Zhu, N. Y.; Yam, V.W.-W. *Organometallics* **2004**, *23*, 3459. (c) Ma, D.-L.; Shum, T.Y.-T.; Zhang, F.; Che, C.-M.; Yang, M. *Chem. Commun*. **2005**, 4675. (d) Wu, P.; Wong, E.L.-M.; Ma, D.-L.; Tong, G.S.-M.; Ng, K.-M.; Che, C.-M. *Chem.—Eur. J*. **2009**, *15*, 3652. (e) Ma, D. L.; Che, C.-M.; Yan, S.-C. *J. Am. Chem. Soc*. **2009**, *131*, 1835.

(5) (a) Botchway, S. W.; Charnley, M.; Haycock, J. W.; Parker, A. W.; Rochester, D. L.; Weinstein, J. A.; Williams, J. A. G. *Proc. Natl. Acad. Sci. U.S.A*. **2008**, *105*, 16071. (b) Koo, C.-K.; Wong, K.-L.; Man, C.W.-Y.; Lam, Y.-W.; So, K.-Y.; Tam, H.-L.; Tsao, S.-W.; Cheah, K.-W.; Lau, K.-C.; Yang, Y.-Y.; Chen, J.-C.; Lam, M.H.-W. *Inorg. Chem*. **2009**, *48*, 872.

(6) Danilov, E. O.; Pomestchenko, I. E.; Kinayyigit, S.; Gentili, P. L.; Hissler, M.; Ziessel, R.; Castellano, F. N. *J. Phys. Chem. A* **2005**, *2465*, 109.

(7) (a) Rausch, A. F.; Thompson, M. E.; Yersin, H. *Chem. Phys. Lett*. **2009**, *468*, 46. (b) Rausch A. F.; Homeier, H. H. H.; Yersin, H. *Top. Organomet. Chem*., **2010**, *29*, 193.

Published on Web 12/11/2009
© 2009 American Chemical Society

The key is normally to make use of ligand-centered (LC) or charge-transfer transitions, while ensuring that d-d excited states, which involve the population of the strongly antibonding $d_{x^2-y^2}$ orbital, are displaced to higher energies not accessible at room temperature.[8] It is probably the thermally activated population of such distorted states that accounts for the lack of room temperature emission in simple complexes like $[Pt(tpy)Cl]^+$, despite the rigidity associated with its terdentate coordination.[9] To raise the energy of d-d states, ligands which exert a stronger ligand-field are required, while retaining rigid architectures. Successful strategies include the replacement of the chloride ligand in $[Pt(tpy)Cl]^+$ by a stronger-field acetylide ($-C\equiv C-Ar$)[10] or cyanide ($-C\equiv N$)[11] ligand, or replacement of the tpy ligand by a cyclometallating analogue such as phbpy or dpyb, both of which approaches result in room temperature emission[12,13] {phbpyH = 6-phenyl-2,2′-bipyridine; dpybH = 1,3-di(2-pyridyl)benzene}.

The reason why tpy itself does not offer sufficient ligand field strength can be traced to the poor bite angle when it binds to large transition metal ions. Thus, the optimal N−Pt−N angle for maximum orbital overlap would be 180°, but the structural constraints of tpy lead to a value of only 163.5(7)° in $[Pt(tpy)Cl]ClO_4$.[14] A similar issue accounts for the well-known difference between $[Ru(tpy)_2]^{2+}$ and $[Ru(bpy)_3]^{2+}$, the former being essentially non-emissive at room temperature owing to a weaker ligand field associated with sublinear N−Ru−N angles of 158.3(3)−159.1(2)°.[15,16]

A potential alternative route to emissive complexes might be to use N^N^N-coordinating ligands which offer a larger bite angle, perhaps involving 6-membered chelation. McMillin and Thummel demonstrated that 2-(8-quinolyl)-1,10-phenanthroline leads to a platinum complex that is significantly emissive in solution at room temperature (Φ_{lum} = 0.002, τ = 310 ns in CH_2Cl_2).[17] This ligand sets up one 5-membered and one 6-membered chelate ring when it binds to Pt(II): the ring strain is hence alleviated and the ligand field increased. Thummel and Hammarström obtained room temperature emissive ruthenium(II) complexes with the same ligand, where the improvement over $[Ru(tpy)_3]^{2+}$ was interpreted similarly.[18] Hammarström and Johannson found that further enhancement of the emission efficiency of $[Ru(N^N^N)_2]^{2+}$ complexes could be achieved with the ligand 2,6-di(8-quinolyl)pyridine, which leads to *two* 6-membered chelates per ligand.[19]

In this contribution, we report on the contrasting influence of 6-membered chelation in N^N^N and N^C^N-coordinated platinum(II) complexes based on 2,6-di(8-quinolyl)-pyridine and 1,3-di(8-quinolyl)benzene. We demonstrate that simple N^N^N complexes are accessible with emission quantum yields comparable to $[Ru(bpy)_3]^{2+}$, whereas a detrimental effect is observed on the luminescence of the N^C^N systems compared to analogues with cyclometalating 5-membered chelate rings. Using the example of an azaindole-based ligand, we also show that favorable geometry alone is not sufficient to ensure good emission properties in N^N^N coordinated systems: electronic factors are obviously also crucial.

Results and Discussion

1. Synthesis of Ligands. The complexes studied are shown in Figure 1, and the strategies employed in the synthesis of the requisite ligands are summarized in Scheme 1. The N^N^N-coordinating ligand 2,6-di-(8-quinolyl)pyridine L^1 was prepared by a Suzuki cross-coupling reaction between 2,6-dibromopyridine and quinoline-8-boronic acid, using the method described by Johannson et al.[20] We found that 2,6-dichloropyridine could also be used, giving a comparable yield of the product. The 4-methoxy derivative L^2 was prepared in a similar manner from 2,6-dibromo-4-methoxypyridine.[21] The preparation of the new N^C^N proligand HL^4 was also carried out by means of a Suzuki cross-coupling reaction, but in this case the functionality in the two units was reversed: 1,3-benzene diboronic acid was coupled with 2 equiv of 8-bromoquinoline.

As an alternative form of N^N^N-chelating ligand, we also investigated L^3, which incorporates 7-azaindole units in place of the 8-substituted quinolines. The combination of copper(I) iodide with *trans*-1,2-diaminocyclohexane, recently established by Buchwald and co-workers as a particularly effective aryl amination catalyst,[22] allowed

(8) (a) Houlding, V. H.; Miskowski, V. M. *Coord. Chem. Rev.* **1991**, *111*, 145. (b) Barigelletti, F.; Sandrini, D.; Maestri, M.; Balzani, V.; von Zelewsky, A.; Chassot, L.; Jolliet, P.; Maeder, U. *Inorg. Chem.* **1988**, *27*, 3644. (c) Williams, J. A. G. *Top. Curr. Chem.* **2007**, *281*, 205.

(9) (a) Crites, D. K.; Cunningham, C. T.; McMillin, D. R. *Inorg. Chim. Acta* **1998**, *273*, 346. (b) McMillin, D. R.; Moore, J. J. *Coord. Chem. Rev.* **2002**, *229*, 113.

(10) (a) Yam, V.W.-W.; Tang, R.P.-L.; Wong, K.M.-C.; Cheung, K.-K. *Organometallics* **2001**, *20*, 4476. (b) Yang, Q.-Z.; Wu, L.-Z.; Wu, Z.-X.; Zhang, L.-P.; Tung, C.-H. *Inorg. Chem.* **2002**, *41*, 5653. (c) Guo, F.; Sun, W.; Liu, Y.; Schanze, K. *Inorg. Chem.* **2005**, *44*, 4055. (d) Chakraborty, S.; Wadas, T. J.; Hester, H.; Flaschenreim, C.; Schmehl, R.; Eisenberg, R. *Inorg. Chem.* **2005**, *44*, 6284. (e) Castellano, F. N.; Pomestchenko, I. E.; Shikhova, E.; Hua, F.; Muro, M. L.; Rajapakse, N. *Coord. Chem. Rev.* **2006**, *250*, 1819. (f) Ziessel, R.; Diring, S.; Retailleau, P. *Dalton Trans.* **2006**, 3285.

(11) Wilson, M. H.; Ledwaba, L. P.; Field, J. S.; McMillin, D. R. *Dalton Trans.* **2005**, 2754.

(12) (a) Cheung, T.-C.; Cheung, K.-K.; Peng, S.-M.; Che, C.-M. *J. Chem. Soc., Dalton Trans.* **1996**, 1645. (b) Neve, F.; Crispini, A.; Campagna, S. *Inorg. Chem.* **1997**, *36*, 6150. (c) Lai, S.-W.; Chan, M.C.-W.; Cheung, T.-C.; Peng, S.-M.; Che, C.-M. *Inorg. Chem.* **1999**, *38*, 4046. (d) Yip, J. H. K.; Suwarno; Vittal, J. J. *Inorg. Chem.* **2000**, *39*, 3537. (e) Shao, P.; Li, Y.; Azenkeng, A.; Hoffmann, M. R.; Sun, W. *Inorg. Chem.* **2009**, *48*, 2407.

(13) (a) Williams, J. A. G.; Beeby, A.; Davies, E. S.; Weinstein, J. A.; Wilson, C. *Inorg. Chem.* **2003**, *42*, 8609. (b) Farley, S. J.; Rochester, D. L.; Thompson, A. L.; Howard, J. A. K.; Williams, J. A. G. *Inorg. Chem.* **2005**, *44*, 9690. (c) Rochester, D. L.; Develay, S.; Záliš, S.; Williams, J. A. G. *Dalton. Trans.* **2009**, 1728. (d) Cocchi, M.; Virgili, D.; Fattori, V.; Rochester, D. L.; Williams, J. A. G. *Adv. Funct. Mater.* **2007**, *17*, 285.

(14) Bailey, J. A.; Hill, M. G.; Marsh, R. E.; Miskowski, V. M.; Schaefer, W. P.; Gray, H. B. *Inorg. Chem.* **1995**, *34*, 4591.

(15) (a) Caspar, J. V.; Meyer, T. J. *Inorg. Chem.* **1983**, *22*, 2444. (b) Juris, A.; Balzani, V.; Barigelletti, F.; Campagna, S.; Belser, P.; von Zelewsky, A. *Coord. Chem. Rev.* **1988**, *84*, 85. (c) Medlycott, E. A.; Hanan, G. S. *Chem. Soc. Rev.* **2005**, *34*, 133.

(16) Lashgari, K.; Kritikos, M.; Norrestam, R.; Norrby, T. *Acta Crystallogr.* **1999**, *C55*, 64.

(17) Hu, Y.-Z.; Wilson, M. H.; Zong, R.; Bonnefous, C.; McMillin, D. R.; Thummel, R. P. *Dalton Trans.* **2005**, 354.

(18) Abrahamsson, M.; Becker, H.-C.; Hammarström, L.; Bonnefous, C.; Chamchoumis, C.; Thummel, R. P. *Inorg. Chem.* **2007**, *46*, 10354.

(19) (a) Abrahamsson, M.; Jäger, M.; Österman, T.; Eriksson, L.; Persson, P.; Becker, H.-C.; Johansson, O.; Hammarström, L. *J. Am. Chem. Soc.* **2006**, *128*, 12616. (b) Abrahamsson, M.; Jäger, M.; Kumar, R. J.; Österman, T.; Persson, P.; Becker, H.-C.; Johansson, O.; Hammarström, L. *J. Am. Chem. Soc.* **2008**, *130*, 15533.

(20) Jäger, M.; Eriksson, L.; Bergquist, J.; Johansson, O. *J. Org. Chem.* **2007**, *72*, 10227.

(21) The method was loosely based on a previously reported procedure: Neumann, U.; Vögtle, F. *Chem. Ber.* **1989**, *122*, 589.

(22) Antilla, J. C.; Baskin, J. M.; Barder, T. E.; Buchwald, S. L. *J. Org. Chem.* **2004**, *69*, 5578.

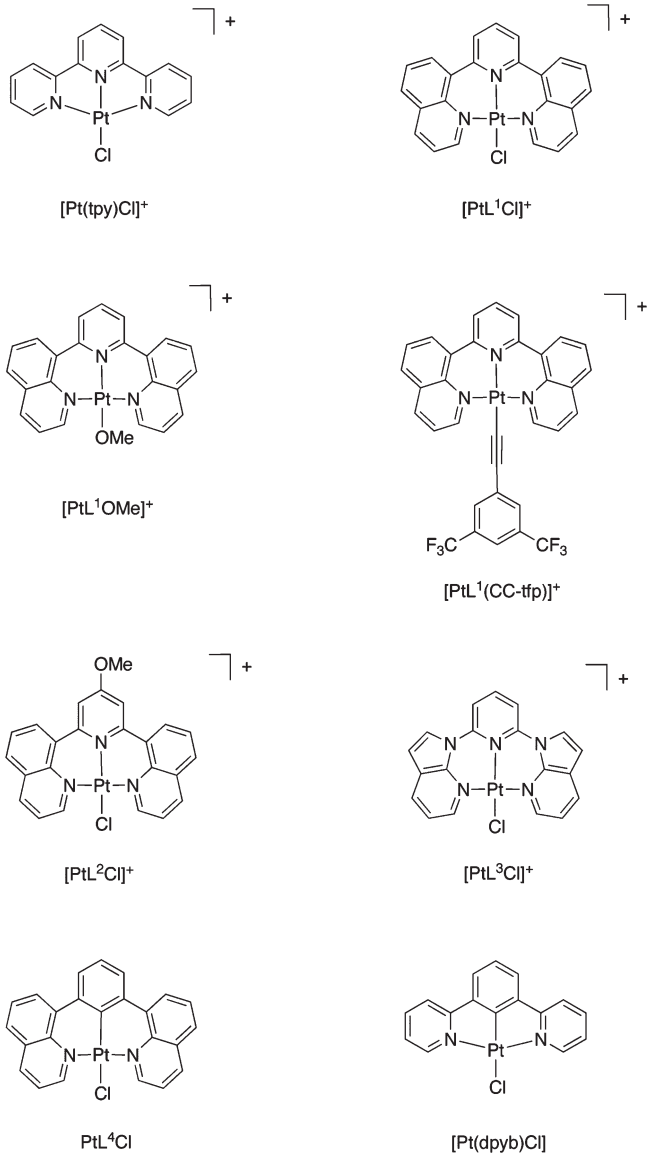

Figure 1. Structural formulas of the complexes investigated in this study. The structures of $[Pt(tpy)Cl]^+$ and Pt(dpyb)Cl are also shown for reference.

coupling of 2,6-dibromopyridine with 2 equiv of 7-azaindole to be carried out under mild conditions to give L^3 in good yield (Scheme 1).

2. Synthesis and Characterization of Platinum(II) Complexes. Complexation of the N^N^N-coordinating ligands to platinum was readily achieved upon treatment with $Pt(DMSO)_2Cl_2$ in refluxing methanol. This simple platinum(II) complex[23] has good solubility in alcohols and does away with the need for water as a co-solvent, which was required when K_2PtCl_4 was used as the platinum precursor. The chloride salts $[PtL^{1-3}Cl]Cl$ were isolated in yields of around 50%, and converted to their hexafluorophosphate salts, $[PtL^{1-3}Cl]PF_6$, upon anion exchange with KPF_6(aq).

The complexation of 2,6-di(quinolyl)pyridine, L^1 to platinum(II) results in shifts to higher frequency of *all* the ^{1}H NMR signals (Figure 2 and Table 1), as typically observed for aromatic ligands when they form cationic

(23) Puddephatt, R. J. *Inorg. Synth.* **2002**, *33*, 189.

Scheme 1. Strategies Employed in the Synthesis of Ligands L^1–L^3 and HL^4[a]

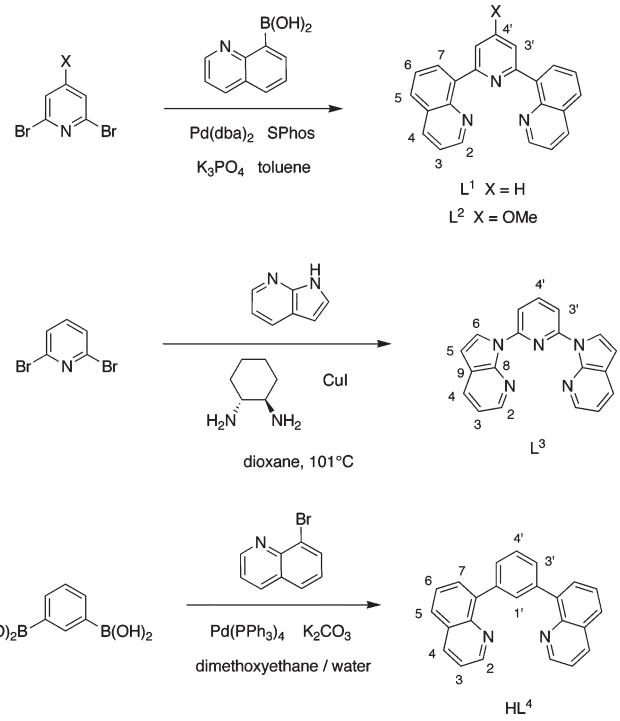

[a] The numbering scheme shown is that used in the assignment of the ^{1}H and ^{13}C spectra. To aid comparison, we number the central ring of HL^4 in the same way as the pyridyl ring in the other ligands.

complexes with square planar geometry. As found for complexation of terpyridine to Pt(II), the protons *para* to the coordinating nitrogen atoms experience a particularly significant deshielding effect ($\Delta\delta \sim 0.5$ ppm). However, the position which experiences the largest perturbation is H^7 of the quinoline, *ortho* to the interannular bond ($\Delta\delta = 0.68$ ppm in d_6-DMSO).

The azaindole ligand L^3 undergoes broadly similar behavior upon complexation, in that most signals also shift to high frequency; however, in this case, position $H^{3'}$ within the central ring experiences a large *shielding* effect of almost 1 ppm (Figure 2 and Table 1). One or both of two possible effects may be involved here. First, the azaindole moiety has σ-withdrawing character but is also a potential π-donor through the indole nitrogen atom. In the uncomplexed ligand, free rotation about the C–N interannular bond may ensure that the former predominates, as conformations close to planarity, which would favor the π-donation, will be sterically disfavored. Upon complexation, the π-donation effect from azaindole to pyridine should increase, as the conformation will become locked. Second, the ligand in the complex is probably not planar but partially twisted (see below). This will lead to $H^{3'}$ being placed within the zone of influence of the diamagnetic ring current of the azaindole. We note that H^6 might in that case be expected to be influenced similarly, and indeed it is the only other signal to experience a shielding effect upon complexation, albeit a smaller one than $H^{3'}$.

The synthesis of the cyclometalated complex PtL^4Cl from ligand HL^4 required a higher temperature to effect the necessary C–H activation. In the ^{1}H NMR spectrum, most of the quinoline resonances are again shifted to

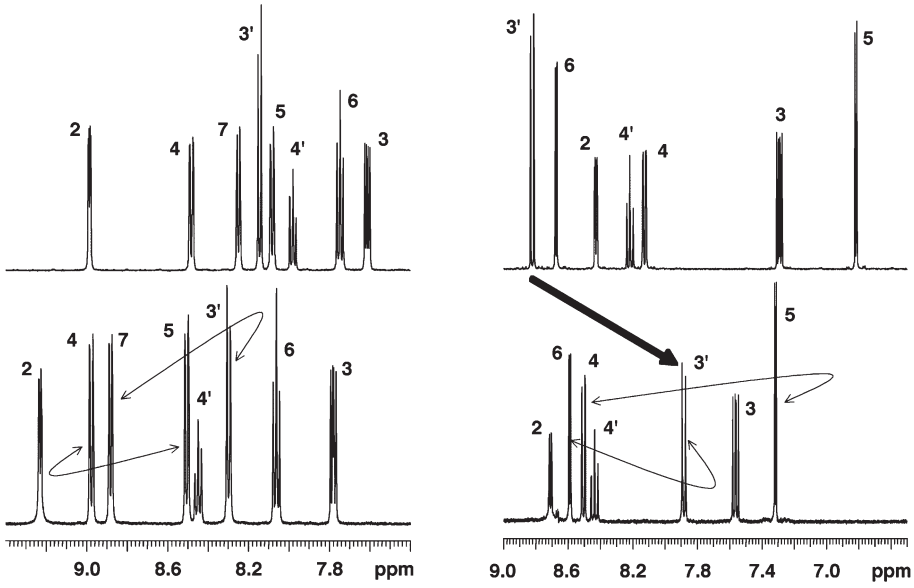

Figure 2. *Left:* ^{1}H NMR spectra of L^1 (top) and $[PtL^1Cl]Cl$ (bottom) in d_6-DMSO at 500 MHz, 298 K. *Right:* Corresponding spectra of L^3 (top) and $[PtL^3Cl]Cl$ (bottom) under the same conditions. Protons are numbered according to Scheme 1. Thin arrows refer to diagnostic NOE couplings. The thick arrow highlights the large upfield shift of the $H^{3'}$ resonance upon complexation.

Table 1. Changes in the ^{1}H NMR Chemical Shifts of the Ligands upon Complexation to Pt(II)

	$[PtL^1Cl]X$			
H^n n = [a]	X = Cl^- [b]	X = PF_6^- [c]	$[PtL^3Cl]Cl$ [b]	PtL^4Cl [d]
2	+ 0.27	+ 0.37	+ 0.29	+ 0.79
3	+ 0.20	+ 0.26	+ 0.39	− 0.06
4	+ 0.53	+ 0.59	+ 0.55	+ 0.20
5	+ 0.52	+ 0.52	+ 0.66	0
6	+ 0.35	+ 0.38	− 0.08	+ 0.09
7	+ 0.68	+ 0.54		+ 0.54
3′	+ 0.18	+ 0.06	− 0.93	− 0.20
4′	+ 0.50	+ 0.57	+ 0.40	− 0.27

[a] Numbering system as in Scheme 1. [b] In d_6-DMSO. [c] In d_6-acetone. [d] In $CDCl_3$.

higher frequency upon complexation, particularly H^2 ($\Delta\delta$ = 0.8 ppm in $CDCl_3$), which also displays well-resolved ^{195}Pt satellites (^3J = 44 Hz). In this case, however, the protons in the central benzene ring experience a shielding effect (Table 1), in line with the increased electron density in the cyclometallating ring that accompanies the Pt−C bond formation. A similar trend has previously been observed for complexes of 1,3-di(2-pyridyl)benzenes.[13]

The methoxide adduct $[PtL^1OMe]^+$ was obtained by treatment of $[PtL^1Cl]PF_6$ with a solution of KOH in methanol at room temperature, and is a distinctly more vivid yellow than the pale starting material. The methoxide protons resonate at 2.82 ppm (in $CDCl_3$), strongly shielded relative to the value for MeOH (3.49 ppm) (spectra are shown in the Supporting Information). Further confirmation of the identity of the product is provided by the Nuclear Overhauser Effect (NOE) seen between this signal and the H^2 protons of the terdentate ligand.

The acetylide derivative $[PtL^1(C{\equiv}C\text{-tfp})]^+$ was prepared by means of a copper-catalyzed metathesis reaction with ethynyl-3,5-bis(trifluoromethyl)-benzene,[24] similar to that used in the preparation of platinum(II) terpyridyl acetylide complexes.[25] The change from chloride to acetylide leads to a large deshielding of the H^2 protons of L^1 in the ^{1}H NMR spectrum ($\Delta\delta$ = +0.5 ppm). No other resonances in L^1 are significantly affected, so this effect is probably through-space in origin, arising from the C−H^2 bonds being parallel and close to the C≡C triple bond of the acetylide.

The identity of all complexes was further confirmed by high-resolution mass spectrometry; a representative example for $[PtL^2Cl]^+$ with isotope matching is provided in Figure S1 of the Supporting Information.

3. Structures of the Complexes by Density Functional Theory. Despite repeated attempts, including the use of different counter-anions in the case of $[PtL^{1-3}Cl]^+$, it has not hitherto proved possible to obtain crystals of the complexes of sufficient quality for an X-ray diffraction study. Density functional theory (DFT) calculations have recently proved highly successful in predicting the structures of metal complexes.[26] When crystal structures have been available for comparison, not only are qualitative trends reproduced well, but there is frequently excellent quantitative agreement in bond lengths and angles.[27] In the present case, we have employed DFT calculations, using an approach now well-established for third row transition metal complexes, to identify the energy-minimized structures (B3LYP functional[28] with double-ζ basis sets, 6-31G for ligands and LANL2DZ for Pt(II),[29] with the inner core electrons of Pt replaced by a relativistic effective core potential).

(24) (a) Sonogashira, K.; Fujikura, Y.; Yatake, T.; Toyoshima, N.; Takahashi, S.; Hagihara, N. *J. Organomet. Chem.* **1978**, *145*, 101. (b) Takahashi, S.; Kuroyama, Y.; Sonogashira, K.; Hagihara, N. *Synthesis* **1980**, 627.

(25) Hissler, M.; McGarrah, J. E.; Connick, W. B.; Geiger, D. K.; Cummings, S. D.; Eisenberg, R. *Coord. Chem. Rev.* **2000**, *208*, 115.

(26) For a recent review of the application of DFT techniques to metal complexes and their excited states, see: Vlček, A.; Záliš, S. *Coord. Chem. Rev.* **2007**, *251*, 258.

(27) Significantly, this is the case for $[RuL^1_2]^{2+}$, where a structure was available to verify the geometry predicted by DFT: see ref 19a.

(28) (a) Becke, A. D. *J. Chem. Phys.* **1993**, *98*, 5648. (b) Lee, C. T.; Yang, W. T.; Parr, R. G. *Phys. Rev. B.* **1988**, *37*, 785.

(29) Hay, P. J.; Wadt, W. R. *J. Chem. Phys.* **1985**, *82*, 270.

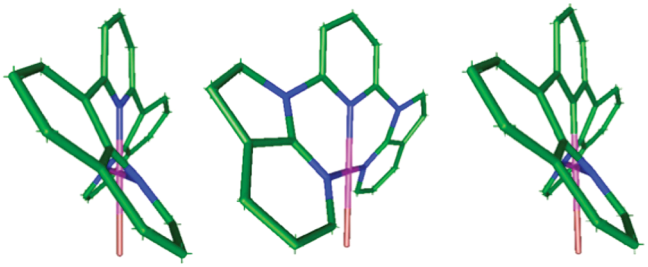

	$[PtL^1Cl]^+$	$[PtL^3Cl]^+$	PtL^4Cl
Interplane angle / °	38.5	28.5	32.6
Trans N–Pt–N angle / °	178.8	178.5	178.5
Lateral N–Pt bond length / Å	2.05	2.05	2.06
Central Pt–N or Pt–C bond length / Å	2.03	2.11	1.99

Figure 3. Structures of complexes $[PtL^1Cl]^+$, PtL^4Cl, and $[PtL^3Cl]^+$ predicted by energy minimization using DFT (gas-phase at 0 K), with the viewing angle selected to best reveal both the twist in the ligand and the planarity at the metal ion. The angle between the planes of the quinoline/azaindole rings and the central pyridine/benzene ring is given, together with the N−Pt−N angle for *trans*-related N atoms. Corresponding angles for $[PtL^1OMe]^+$ are 31.6° and 174.9°, and for $[PtL^1(C{\equiv}C\text{-tfp})]^+$ 34.1° and 179.7°. Key bond lengths are also indicated.

Figure 3 shows the structures obtained in this way for the three classes of compound. In each case, it is clear that the ligand is not planar: on the contrary, there is a significant twisting of the planes of the lateral quinoline/azaindole rings relative to the central pyridyl/benzene ring. Such a twisting is intuitively reasonable, since the platinum ion would be too large to bind to the ligand in a planar conformation, and the bite angle of the ligand would be inappropriate. By rotation of the plane of the lateral heterocyclic rings relative to that of the central ring, the d^8 metal ion achieves its preferred square planar coordination. The torsion angles between the planes are shown in Figure 3; the angle is smallest for the complex of the azaindole ligand $[PtL^3Cl]^+$.

Importantly, it can be seen that the N−Pt−N angle (for the *trans*-related, quinolyl nitrogen atoms) is close to 180° in each case, suggesting that the strategy of employing 6-membered chelate rings is successful in relieving the strain associated with the more acute angles subtended by 5-membered-chelate-forming ligands such as terpyridine. A similar twisting of the ligands was observed for $[RuL^1{}_2]^{2+}$ by Hammarström, Johansson, and co-workers, leading to a geometry close to pure octahedral at the metal (intraligand *trans* N−Ru−N angles are 177.6(7)° determined by X-ray diffraction).[19a] Only for the methoxide adduct $[PtL^1OMe]^+$ is there a significant (though still quite small) deviation from linearity: the angle here is 174.9°. In contrast to terpyridyl complexes, this deviation is caused by displacement of the metal ion toward the central ring, that is, such that $N^{py}-Pt-N^{quin} > 90°$.

4. Electrochemistry of the Complexes and Frontier Orbital Description. The cationic complexes $[PtL^{1-3}Cl]^+$ and derivatives $[PtL^1OMe]^+$ and $[PtL^1(C{\equiv}C\text{-tfp})]^+$ were investigated by cyclic voltammetry in acetonitrile solution, in the presence of Bu_4NPF_6 (0.1 M) as the supporting electrolyte; data are reported in Table 2 relative to ferrocene under the same conditions ($E_{1/2}{}^{ox}$ = 0.40 V vs SCE[30]). Each complex displays an irreversible oxidation in the region 0.6−0.8 V, which is tentatively attributed to a metal-based oxidation process. Typically, Pt(II) complexes with di- and tri-imines and related ligands either do not display clear-cut oxidations, or, if they do so, they are normally irreversible, owing to the reactivity of Pt(III) at the vacant axial sites.[31] DFT supports the notion that the metal is involved in the oxidation: the calculated highest-occupied molecular orbital (HOMO) of each complex (Figure 4) is composed almost exclusively of metal and co-ligand (Cl, OMe, or acetylide) orbitals.

The cationic quinolyl complexes display two partially reversible reduction processes in the cyclic voltammetry, most likely involving the π^* orbitals of the terdentate ligand. The reduction potentials for $[PtL^{1-2}Cl]^+$ are similar to those displayed by $[Pt(tpy)Cl]^+$ (Table 2), where terpyridine-based reduction is well-established.[9,32] The LUMO (lowest unoccupied molecular orbital) and LUMO+1 of these complexes calculated by DFT are indeed based almost exclusively on the terdentate ligand, spanning all five aromatic ring moieties, and with essentially no contribution from the metal or co-ligand (Figure 4 and Figure S3 in Supporting Information). Strikingly, however, the first reduction process in the azaindole complex $[PtL^3Cl]^+$ is cathodically displaced relative to its quinolyl analogue by >1 V. This observation is consistent with a simplistic picture of the azaindole unit being much more electron-rich than a quinoline: for example, in its reactivity, azaindole behaves as an indole, susceptible to electrophilic attack, rather than as a quinoline. The picture is further supported by the DFT calculations, which reveal that the LUMO in this complex is localized on the central pyridine ring of the ligand, with essentially no contribution from the lateral rings (Figure 4), and in stark contrast to the delocalized nature of the LUMO in the quinolyl complexes.

(30) Connelly, N. G.; Geiger, W. E. *Chem. Rev.* **1996**, *96*, 877.

(31) Only when there is some protection against such reactivity are reversible oxidative processes observed; e.g., Klein, A.; Kaim, W. *Organometallics* **1995**, *14*, 1176.

(32) Rakhimov, R. D.; Weinstein, Y. A.; Lileeva, E. V.; Zheligovskaya, N. N.; Mel'nikov, M. Y.; Butin, K. P. *Russ. Chem. Bull.* **2003**, *52*, 1150.

Table 2. Ground State UV-Visible Absorption and Electrochemical Data of the Platinum(II) Complexes in Solution at 298 K, and the Predominant Character and Energy of the Lowest-Lying Singlet State Obtained by TD-DFT

complex	absorption λ_{max}/nm [a] ε/M^{-1} cm^{-1}	lowest S state E/eV [λ/nm]	E^0_{ox}/V [b]	E^0_{red}/V [b] (Δ/mV)
$[Pt(tpy)Cl]^+$	305, 320, 340, 390, 403 [c]			−1.24 (70), −1.82 (70)[c]
$[PtL^1Cl]^+$	240 (67 200), 327sh (23 200), 347 (26 100)	HOMO→LUMO 2.99 [415]	0.67	−1.27 (160), −1.78
$[PtL^1(OMe)]^+$	274 (81 400), 350 (28 500), 405 (4 860)	HOMO→LUMO 2.44 [508]	0.77	−1.41 (120), −1.98
$[PtL^1(C{\equiv}C\text{-}tfp)]^+$	239 (64 700), 271 (34 300), 349 (24 200), 364 (21 500)	HOMO→LUMO 2.45 [506]	0.78	−1.49 (100), −1.66
$[PtL^2Cl]^+$	238 (76 800), 274 (25 000), 337 (24 000)		0.83	d
$[PtL^3Cl]^+$	265 (55 700), 336 (16 800)	HOMO→LUMO 3.38 [366]	0.62	−2.73
PtL^4Cl	320 (67 500), 356 (49 900), 420 (31 500)	HOMO→LUMO 2.61 [475]	0.62 [e]	−1.57 (80), −2.26 (160)
Pt(dpyb)Cl	332 (6510), 380 (8690), 401 (7010), 454 (270), 485 (240) [e]		0.35[e,f]	−2.14[e,f]

[a] In solution in CH_2Cl_2. [b] In solution in MeCN except where indicated otherwise, using Bu_4NPF_6 (0.1 M) as the supporting electrolyte. Peak potentials are given for the irreversible oxidations and second reductions where return wave was ill-defined. For the pseudo-reversible reductions, values refer to $E_{1/2}$ and the peak-to-peak separation is given in parentheses. Values refer to a scan rate of 300 mV s^{-1} and are reported relative to Fc^+|Fc. [c] Data from refs 14 and 9a. [d] The reduction wave was poorly defined for this complex. [e] In CH_2Cl_2. [f] Data from ref 13a.

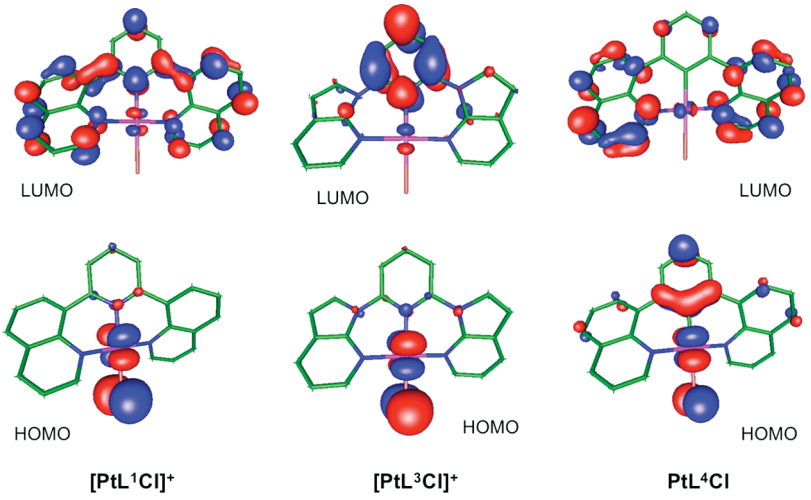

Figure 4. Frontier orbitals of complexes $[PtL^1Cl]^+$, $[PtL^3Cl]^+$, and PtL^4Cl calculated by TD-DFT.

The electrochemistry of the cyclometalated complex PtL^4Cl was examined in dichloromethane solution, owing to poor solubility in MeCN. As for the N^N^N analogue $[PtL^1Cl]^+$, an irreversible oxidation and two reduction processes were observed. A quantitative comparison of the potentials is undermined by the use of a different solvent, but all the potentials are shifted to less positive/more negative values, consistent with the more electron-rich character expected for this charge-neutral, cyclometalated complex. In this case, the HOMO calculated by DFT shows not only Pt(5d) and Cl(p) character but also a significant contribution from the central phenyl ring (Figure 4), whose electron density will be raised as a result of the deprotonation that accompanies cyclometalation. Conversely, this ring plays much less role in the LUMO than the pyridyl ring in the N^N^N complexes, and the LUMO becomes essentially localized on the lateral quinoline moieties. Thus the picture is, in effect, the reverse of that found in the complex of the azaindole ligand L^3. A broadly similar trend of significant participation of the cyclometallating ring in the HOMO, but relatively low contribution to the LUMO, has also been observed in TD-DFT studies of Pt(dpyb)Cl and its derivatives.[13c,33]

5. Photophysical Properties. (a). Absorption. The absorption spectra of representative complexes in dilute solution in dichloromethane at room temperature are shown in Figure 5, and data for all the complexes are compiled in Table 2. Additional spectra are provided in the Supporting Information. Each complex displays a set of intense bands at high-energy (< 280 nm), at least some of which can be attributed to $\pi-\pi^*$ transitions within the ligands, as they display bands in the same region. For consideration of lower-energy features, we divide the complexes into three groups:

(i). $[PtL^1X]^+$ (X = Cl, OMe, C≡C-tfp), and $[PtL^2Cl]^+$. A band or, more likely, an envelope of several close bands around 350 nm, has no counterpart in the uncoordinated ligands. They show only a very small degree of negative solvatochromism (e.g., Supporting Information, Figure S5). These bands are anticipated to arise from charge-transfer transitions involving the metal and/or co-ligand, by comparison with other established platinum di- and tri-imine complexes.[9,8c] Time-dependent DFT (TD-DFT) calculations reveal that the lowest-lying spin-allowed singlet state is composed mainly of HOMO→LUMO character in each case. Hence, it is appropriate to consider the frontier orbital pictures of Figure 4 in interpreting the nature of the lowest-energy bands in the absorption spectra. They suggest that the lowest-energy band be assigned as charge-transfer from the metal and monodentate co-ligand X to the tridentate ligand, $d(Pt)/\pi(X) \rightarrow \pi^*(N^\wedge N^\wedge N)$. The lack of significant solvatochromism can be understood in terms of the movement of electron density from the central axis of the

(33) Sotoyama, W.; Satoh, T.; Sato, H.; Matsuura, A.; Sawatari, N. *J. Phys. Chem. A* **2005**, *109*, 9760.

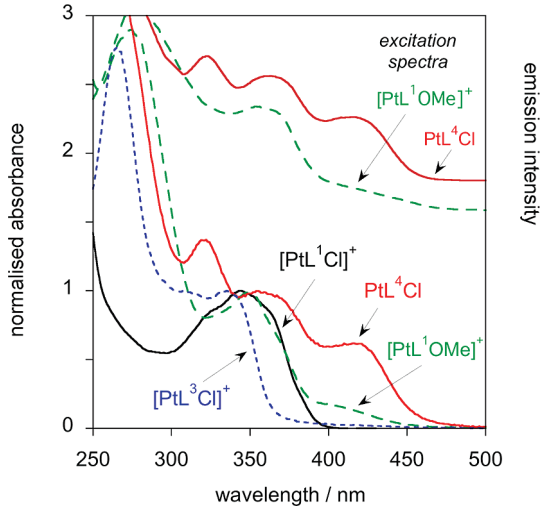

Figure 5. Normalized UV−visible absorption spectra of the Pt(II) complexes in CH_2Cl_2 at 298 K. The spectra of $[PtL^1(C{\equiv}C\text{-tfp})]^+$ and $[PtL^2Cl]^+$ are omitted here for clarity; they are provided in Figure S4 of the Supporting Information, and data is summarized in Table 2. Inset: excitation spectra of $[PtL^1OMe]^+$ and PtL^4Cl (λ_{em} = 600 nm) in CH_2Cl_2 at 298 K.

molecule outward toward the quinolyl rings, rather than from one end of the molecule to the other, such that the change in dipole moment accompanying excitation will be minimal.

The absorption spectrum of the methoxy-substituted complex $[PtL^2Cl]^+$ is similar to that of $[PtL^1Cl]^+$, but a little shifted to the blue, probably reflecting destabilization of the LUMO by the electron-donating effect of the substituent (see Figure S4 in Supporting Information for spectrum).

In the case of the methoxide derivative, the lowest-energy band is a shoulder at 405 nm, having apparently emerged from under the envelope of bands centered around 350 nm (Figure 5). Qualitatively, this would be consistent with the notion that the methoxide co-ligand is a stronger σ-donor than chloride, such that the energy of the CT state will be reduced. The difference in energy relative to the center of the band in $[PtL^1Cl]^+$ (λ_{max} = 347 nm) is around 4400 cm^{-1}.

Meanwhile, the energies of the S_1 excited states predicted by TD-DFT are listed in Table 2. Although the absolute values are underestimated compared to the experimental ones in all cases, consideration of the trends is informative. Indeed, for $[PtL^1OMe]^+$ compared to $[PtL^1Cl]^+$, there is a difference of 0.54 eV or 4400 cm^{-1}, which agrees remarkably well with the experimental value. The possibility that the low-energy band is due to a dimer or aggregate, leading to a $Pt_2(\sigma^*) \rightarrow \pi^*(N^\wedge N^\wedge N)$ MMLCT transition[34] for example, can be ruled out, because (i) the profile of the absorption spectrum is independent of concentration (the range up to 10^{-4} M was investigated), and (ii) the bands also appear in the luminescence excitation spectrum (see Figure 5 and Section 5b). The TD-DFT calculations also suggest that a similar low-energy transition should be observed in $[PtL^1(C{\equiv}C\text{-tfp})]^+$. Although less clear-cut than for the methoxide adduct, the experimental absorption spectrum does reveal a tail on the red end of the spectrum of the acetylide adduct compared to the parent chloro complex (Figure S4, Supporting Information).

(ii). $[PtL^3Cl]^+$. The complex of the azaindole ligand similarly displays a quite broad band, but at higher energy, λ_{max} = 336 nm. Again the TD-DFT indicates that the lowest-lying singlet state has primarily HOMO→LUMO character. The higher energy of the band can then be understood in terms of the destabilized LUMO, as evident from the more negative reduction potential of this complex (vide supra) and from the molecular orbital plot of the LUMO in Figure 4, which was seen to be largely localized on the pyridine ring rather than being delocalized across the N^N^N ligand.

(iii). PtL^4Cl. The cyclometalated complex has a pronounced band at lower energy ($\lambda_{max} \sim$ 420 nm) than its N^N^N-coordinated analogue $[PtL^1Cl]^+$. This is fully consistent with cyclometalation, which tends to raise the energy of the HOMO owing to the increased electron density, as discussed in section 4: the substantial participation of the central metalated ring in the HOMO is shown in Figure 4. The TD-DFT data (Table 2) confirms that a significantly lower S_1 energy is expected for this complex compared to $[PtL^1Cl]^+$ (difference of 0.38 eV). The band displays a larger degree of solvatochromism than $[PtL^1Cl]^+$ (Supporting Information, Figure S6).

We note that in none of these complexes is there evidence for any lower energy bands arising from the direct S→T transition. This is in contrast to Pt(dpyb)Cl and derivatives, for example, where relatively weak but distinct low-energy bands in the absorption spectrum ($\varepsilon \sim$ 200) arise from direct excitation to the triplet state facilitated by spin-coupling associated with the Pt(II) ion.[13,35] It suggests that the oscillator strength for these spin-forbidden transitions is small in the present set of complexes. We return to this point in the next section.

(b). Emission. All of the quinolyl complexes are luminescent in solution at room temperature; data are compiled in Table 3 and representative spectra are shown in Figure 6.

(i). $[PtL^1Cl]^+$. $[PtL^1Cl]^+$ displays a broad, unstructured emission profile centered at 600 nm. The emission displays no significant solvatochromism: the spectra recorded in tetrahydrofuran (THF), $CHCl_3$, and MeCN are superimposable with the spectrum in CH_2Cl_2 under the same conditions. The quantum yield of luminescence in solution is 0.036 (degassed CH_2Cl_2, 298 K), a value comparable to that of such archetypal transition metal complexes as $[Ru(bpy)_3]^{2+}$, and, strikingly, vastly superior to that of the terpyridyl analogue $[Pt(tpy)Cl]^+$, from which emission can scarcely be detected under these conditions.[9] The luminescence decay follows monoexponential kinetics, with a lifetime of 16 μs, indicative of emission emanating from a triplet state promoted by the spin−orbit coupling associated with the Pt(II) center. No significant self-quenching was observed upon increasing the concentration from 5×10^{-6} to 10^{-4} M. At 77 K in a frozen glass, the emission becomes highly structured with a vibrational progression of ~1300 cm^{-1} (Figure 7).

(34) Miskowski, V. M.; Houlding, V. H.; Che, C.-M.; Wang, Y. *Inorg. Chem.* **1993**, *32*, 2518.

(35) Rausch, A. F.; Murphy, L.; Williams, J. A. G.; Yersin, H. *Inorg. Chem.* **2009**, *28*, 11407.

Table 3. Luminescence Data for the Platinum Complexes in CH_2Cl_2 Solution at 298 K except Where Stated Otherwise

complex	emission λ_{max}/nm	$\Phi_{lum} \times 10^2$	τ/μs degassed (aerated)	$k^{Q}_{O2}/10^8$ M^{-1} s^{-1a}	$k_r/10^3$ s^{-1b}	$\sum k_{nr}/10^4$ s^{-1b}	emission 77 K[c] λ_{max}/nm	emission 77 K[c] τ/μs
$[Pt(tpy)Cl]^+$	500, 535, 590[d]	0.04[d]	< 0.01 [d]		40	10^4	476, 510, 543, 588[d,e]	13.3[d,e]
$[PtL^1Cl]^+$	600	3.6	16 (1.1)	3.8	2.3	6.0	538, 579, 623	130
$[PtL^1(OMe)]^+$	612	0.7	1.3 (0.58)	4.3	5.4	76	544, 587, 628	70
$[PtL^1(C{\equiv}C\text{-}tfp)]^+$	593	4.2	33 (0.69)	6.4	1.3	2.9	537, 578, 622	135
$[PtL^2Cl]^+$	558(sh), 594	1.0	7.3 (0.94)	4.2	1.4	14	535, 572, 616	160
$[PtL^3Cl]^+$	f						451, 483, 519	460
PtL^4Cl	611(sh), 645	1.6	14 (f)		1.1	7.0	575, 626, 676	28
Pt(dpyb)Cl	491, 524, 562	60[g]	7.2 (0.5)[g]	9.1[g]	83	5.6	492, 525, 562	7.0

[a] k^{Q}_{O2} is the bimolecular rate constant for quenching by molecular oxygen at 298 K, estimated from the lifetime in degassed and aerated solutions, assuming $[O_2]$ at 1 atm pressure of air = 2.2 mmol dm^{-3}. [b] k_r and $\sum k_{nr}$ are the radiative and non-radiative rate constants estimated from the quantum yield and lifetime at 298 K. [c] In diethylether/isopentane/ethanol, except where stated otherwise. [d] Data from ref 9a. [e] In ethanol/methanol/dimethylformamide 5:5:1 (EMD) at 70 K. [f] Emission too weak to be detected using available instrumentation. [g] Data from ref 13a.

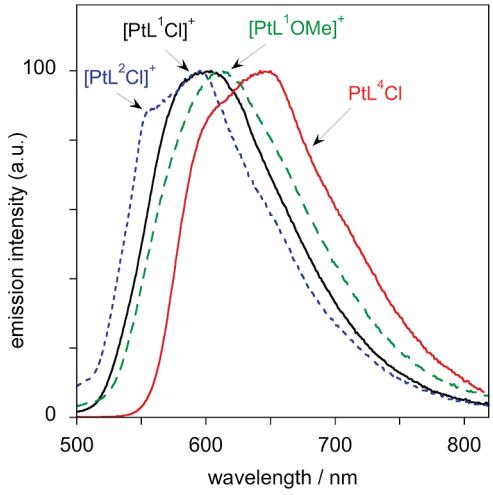

Figure 6. Emission spectra of selected Pt(II) complexes in CH_2Cl_2 at 298 K, following excitation into the lowest-energy absorption band. The spectrum of $[PtL^1(C{\equiv}C\text{-}tfp)]^+$, omitted here for clarity, is provided in Figure S8 of the Supporting Information; see also Table 3.

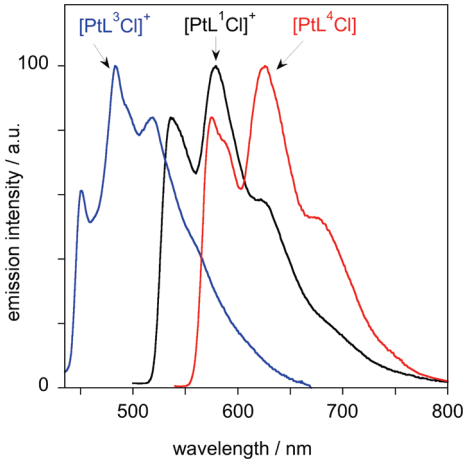

Figure 7. Emission spectra of $[PtL^1Cl]PF_6$, $[PtL^3Cl]PF_6$, and PtL^4Cl at 77 K in a diethyl ether/isopentane/ethanol (2:2:1 v/v) glass. The spectra of the other complexes are omitted for clarity, but are very similar to that of $[PtL^1Cl]^+$, being only slightly blue- and red-shifted respectively for $[PtL^2Cl]^+$ and $[PtL^1OMe]^+$, see Figure S7 in the Supporting Information.

The respectable luminescence quantum yield and long lifetime at room temperature indicate that non-radiative decay pathways have been greatly reduced in the new complex compared to its terpyridyl analogue. The starting hypothesis that the increased chelate ring size should reduce the ring strain, leading to a stronger ligand field and displacement of potentially deactivating d-d states to higher energy, thus appears to be vindicated.[36]

In interpreting the above observations, it is informative to estimate the radiative rate constant (k_r) and the sum of the non-radiative decay constants ($\sum k_{nr}$) from the quantum yields and lifetimes. Although this approach assumes that the emitting state is formed with unitary efficiency—almost certainly incorrect given recent observations of time-zero fluorescence in third row transition metal complexes[37]—it is probably nevertheless a reasonable approximation to make, especially given the good match between the excitation and absorption spectra. The value of $\sum k_{nr}$ obtained in this way is comparable to that for Pt(dpyb)Cl and derivatives, one of the most emissive class of platinum complexes known ($\Phi > 0.6$),[8c] suggesting that the 6-membered chelate strategy is comparable to cyclometalation in terms of reducing non-radiative decay pathways.

On the other hand, the factor limiting the quantum yield of $[PtL^1Cl]^+$ is seen to be the relatively small radiative rate constant k_r, which is well over an order of magnitude lower than for Pt(dpyb)Cl and some 2 orders of magnitude less than the brightest iridium-based emitters such as $Ir(ppy)_3$.[38] The lack of observable low-energy transitions to the triplet state in the absorption spectrum (vide supra) similarly indicates a low oscillator strength for the S→T transition. Low radiative rate constants and oscillator strengths may reflect a relatively low participation of the metal in the excited state, being typical for ligand-centered (^{3}LC, $\pi-\pi^*$) transitions, since it is the spin−orbit coupling associated with the metal ion that promotes the formally spin-forbidden transitions.

(36) A larger gap between the emissive state and the d-d state could also be explained simply on the basis that the emissive state in $[PtL^1Cl]^+$ is lower in energy than in $[Pt(tpy)Cl]^+$, and might not necessarily mean that the d-d state has been raised in energy. However, we note that the new complex is significantly brighter than complexes with tpy derivatives that emit at similar energies; e.g., see refs 9 and 8c for examples.

(37) (a) Cannizzo, A.; Blanco-Rodriguez, A. M.; El Nahhas, A.; Sebera, J.; Záliš, S.; Vlček, A.; Chergui, M. *J. Am. Chem. Soc.* **2008**, *130*, 8967. (b) Hedley, G. J.; Ruseckas, A.; Samuel, I. D. W. *J. Phys. Chem. A* **2009**, *113*, 2.

(38) Flamigni, L.; Barbieri, A.; Sabatini, C.; Ventura, B.; Barigelletti, F. *Top. Curr. Chem.* **2007**, *281*, 143.

A ligand-centered assignment is supported by the observed absence of solvatochromism in the emission spectrum. The highly structured form of the emission at 77 K and its resemblance to that of the phosphorescence of the uncoordinated ligand L^1 (Table 4 and Figure S10 in the Supporting Information) also supports the notion that a predominantly ligand-centered assignment may be appropriate.

Hammarström, Johansson, and co-workers similarly found that non-radiative decay was greatly decreased in $[RuL^1{}_2]^{2+}$ compared to $[Ru(tpy)_2]^{2+}$, attributed to the less strained coordination geometry.[19] In that case, however, the broad, structureless emission band appeared at much lower energy (λ_{max} = 700 nm at 298 K; 673 nm at 77 K). An unequivocal MLCT assignment is clear-cut in that instance. The lower energy of the atomic d orbitals of Pt(II) compared to Ru(II) would account for the greater LC character of the Pt complex.

(ii). $[PtL^2Cl]^+$, $[PtL^1OMe]^+$, and $[PtL^1\text{-}C{\equiv}C\text{-}tfp]^+$. The acetylide adduct displays an emission spectrum very similar to that of the parent chloro complex. The spectrum of the methoxide adduct is also similar but marginally red-shifted compared to $[PtL^1Cl]^+$, while that of $[PtL^2Cl]^+$ is a little blue-shifted and shows a hint of structure (Figure 6). In a frozen glass at 77 K, all four complexes display very similar spectra (Figure S7 in the Supporting Information). The similarity between the spectra offers further support for a predominantly ligand-centered assignment to the emissive state in these complexes, since the co-ligand is seen to have little influence on the triplet excited state energy. Again, there is essentially no solvatochromism in fluid solution (Supporting Information, Figure S8), supporting the LC assignment.

Changing the co-ligand does, however, affect the luminescence lifetime; in particular, the value is increased to 33 μs for the acetylide adduct, apparently reflecting both reduced radiative and non-radiative decay rates (Table 3), while the methoxide adduct has the shortest lifetime and lowest quantum yield among the four complexes, owing to substantially increased non-radiative decay.

(iii). $[PtL^3Cl]^+$. No emission could be detected from this complex in degassed solution at room temperature. At 77 K, a weak, structured emission spectrum could be recorded (Figure 7), blue-shifted substantially compared to the other cationic complexes: $\lambda_{max}{}^{0-0}$ = 451 nm. The higher-energy of the emissive excited state is fully consistent with the conclusions of the absorption, electrochemical, and TD-DFT data discussed above, interpreted in terms of a destabilized ligand π^* LUMO in this complex. The luminescence lifetime of 460 μs at 77 K is much longer than for any of the other complexes, suggesting that the radiative rate constant is low. Meanwhile, the proportionally higher intensity of the 0−1 and 0−2 vibrational bands relative to the 0−0 in $[PtL^3Cl]^+$ compared to the other complexes (i.e., larger Huang−Rhys factor) suggests that the formation of the excited state is accompanied by more distortion than in the other complexes. One might tentatively propose that the binding angle of L^3 may be less appropriate than in the other complexes, being adversely affected by the more acute angle associated with the five-membered pyrrolic ring of the azaindole unit, compared to the six-membered benzenoid ring of the quinolines. We note that, in adopting the linear N−Pt−N geometry for the trans-disposed nitrogens, the predicted Pt−N bond length for the *central* N becomes longer than optimal (2.11 Å compared to 2.05 Å in $[PtL^1Cl]^+$, Figure 3), no doubt reducing the rigidity and ligand field strength. Both factors will lead to faster non-radiative decay in fluid solution. Meanwhile, the higher-energy of the emissive state in this case necessarily reduces the energy gap to the higher-lying d-d states, potentially also promoting deactivation. Coupled with the smaller k_r value, these factors probably account for the lack of emission at room temperature. We note that Wang and co-workers have explored N^C^N-coordinating ligands based on the 7-azaindole unit,[39] and similarly found that their Pt(II) complexes were non-emissive at room temperature.[40]

Table 4. Phosphorescence Maxima and Lifetimes (in EPA at 77 K) of Ligands L^{1-3} and HL^4

ligand	emission λ_{max}/nm	τ/ms
L^1	496, 532, 570	490
L^2	492, 528, 568	600
L^3	428, 442, 459, 474, 485	2400
HL^4	503, 536, 574	560

(iv). PtL^4Cl. The cyclometalated complex emits in degassed solution at room temperature: λ_{max} = 645 nm, τ = 14 μs, Φ = 0.016 in CH_2Cl_2. The emission maximum is red-shifted relative to the cationic quinolyl complexes (Figure 6). There is a hint of vibrational structure in the spectrum in the form of a higher-energy shoulder, similar to that displayed by $[PtL^2Cl]^+$. Again, there is essentially no solvatochromism (Supporting Information, Figure S9). At 77 K, the red-shift is more clear-cut. The spectrum at this temperature has a profile essentially identical to that of the cationic quinolyl complexes, but is shifted to lower-energy by ~1200 cm^{-1} (Figure 7). As in absorption, it is reasonable to ascribe the lower excited state energy to a destabilized HOMO arising from the effect of cyclometalation. This interpretation, in terms of a greater influence of the metal in the excited state of the cyclometalated compound compared to the N^N^N complex, is reinforced by the observation that the *uncomplexed* ligands L^1 and HL^4 have emission spectra at 77 K that are essentially identical to one another (Supporting Information, Figure S10).

It is pertinent to compare the emission properties of PtL^4Cl with those of Pt(dpyb)Cl, the analogous complex incorporating pyridyl rings (coordinating through 5-membered chelates) rather than quinolines. The former has a substantially lower luminescence quantum yield and longer luminescence lifetime than the latter at room temperature. The difference seems to be due primarily to the lower radiative rate constant of PtL^4Cl. The value of 1100 s^{-1} (Table 3) is around 2 orders of magnitude less than that for Pt(dpyb)Cl, while the non-radiative decay is of a similar order in the two complexes. Recent cryogenic studies (T = 1.2−4 K) have revealed the presence of efficient spin−orbit coupling pathways in Pt(dpyb)Cl, despite the apparent "LC-like" nature of the emission.[35]

(39) Wu, Q.; Lavigne, J. A.; Tao, Y.; D'Iorio, M.; Wang, S. *Chem. Mater.* **2001**, *13*, 71.
(40) Song, D.; Wu, Q.; Hook, A.; Kozin, I.; Wang, S. *Organometallics* **2001**, *20*, 4683.

Apparently, spin−orbit coupling is less efficient in the quinolyl-based complex than in the pyridyl analogue, but more detailed studies of PtL^4Cl at such temperatures will be required to unravel the origins of this difference.

Concluding Discussion and Summary

In this study, we have prepared new complexes of platinum with terdentate ligands incorporating 8-substituted quinolines or 7-N-substituted azaindoles as the lateral coordinating units. The energy-minimized geometries predicted by DFT reveal that, by twisting away from planarity, these ligands are able to bind to platinum in a terdentate manner, in such a way that the N−Pt−N angle is close to 180°. This contrasts with the smaller angle of around 163° observed in $[Pt(tpy)Cl]^+$ and derivatives. The ability to bind linearly, while similar bond lengths are retained, is expected to lead to an increase in the ligand-field strength exerted by the terdentate ligand.

For the N^N^N-coordinating complexes based on the quinolyl ligands ($[PtL^1Cl]^+$ and $[PtL^2Cl]^+$), a dramatic difference in photophysical properties is observed compared to $[Pt(tpy)Cl]^+$. Whereas the photoluminescence of the latter is scarcely detectable in solution at room temperature, $[PtL^1Cl]^+$ emits quite brightly, with a quantum yield of 3.6%. The difference may be due to the displacement of the potentially deactivating d-d states to higher energy, as a result of the stronger predicted ligand field. A number of observations (relatively long luminescence lifetimes, low radiative rate constants, lack of solvatochromism, vibrationally structured emission spectra at 77 K that have little dependence on the identity of the co-ligand) suggest that the emission emanates from a triplet state of predominant ligand-centered character.

In contrast, no emission can be detected from the N^N^N-coordinated complex based on the azaindole ligand $[PtL^3Cl]^+$, despite a similar linear N−Pt−N geometry predicted in this case. Clearly, unstrained geometry alone is not sufficient to confer good emissive properties. The electronic properties appear to be such that the triplet radiative decay rate is not promoted to the same extent as in the other complexes, as manifest by the particularly long luminescence lifetime at 77 K. Non-radiative decay is also likely to be increased in this complex, owing to a less rigid structure and a longer Pt−py bond.

Finally, the cyclometalated, N^C^N-coordinated complex PtL^4Cl proves to be emissive, but in this case, the efficiency is reduced relative to the analogous pyridyl-based complex with 5-membered chelates, apparently because of the triplet radiative transition being less allowed.

Are terdentate ligands that form 6-membered chelate rings better, from the point of view of promoting luminescence of their platinum complexes, than those which conventionally form 5-membered ones? Clearly, the study reveals that such ligands may be preferable, but are not necessarily so. As usual, a variety of factors, geometric and electronic, are involved in determining luminescence quantum yields. In the case of the N^N^N-coordinating quinolyl ligands, performance is certainly enhanced, and the study may open up a range of possibilites with this new class of emissive complexes.

Experimental Section

^1H and ^{13}C NMR spectra, including NOESY and COSY, were recorded on Varian or Bruker spectrometers operating at the frequencies indicated. Chemical shifts (δ) are in parts per million, referenced to residual protio-solvent resonances, and coupling constants are in hertz. Electrospray ionization mass spectra were acquired on a time-of-flight Micromass LCT spectrometer. All solvents used in preparative work were at least Analar grade, and water was purified using the Purite system. Solvents used for optical spectroscopy were HPLC grade.

2,6-Di(8-quinolyl)pyridine L^1. This compound was initially prepared from 2,6-dibromopyridine and quinoline-8-boronic acid as reported previously by Johansson and co-workers.[19a,20] We note that the reaction proceeded equally well from 2,6-dichloropyridine, using an otherwise identical procedure. ^1H NMR data has previously been reported in $CDCl_3$.[19a] To assist comparison with the spectra of the Pt(II) complexes, we report here data in other pertinent solvents. ^1H NMR (400 MHz, d_6-acetone): δ = 9.00 (2H, dd, ^3J = 4.0, ^4J = 1.5, H^2), 8.43 (4H, overlapping dd, H^4 and H^7), 8.34 (2H, d, ^3J = 8.0, $H^{3'}$), 8.05 (2H, dd, ^3J = 7.0, ^4J = 1.5, H^5), 7.97 (1H, t, ^3J = 8.0, $H^{4'}$), 7.75 (2H, dd, ^3J = 8.5, ^3J = 7.0, H^6), 7.58 (2H, dd, ^3J = 8.0, ^3J = 4.0, H^3). ^1H NMR (400 MHz, d_6-DMSO): δ = 8.98 (2H, dd, ^3J = 4.0, ^4J = 1.5, H^2), 8.48 (2H, dd, ^3J = 7.0, ^4J = 1.5, H^4), 8.24 (2H, dd, ^3J = 7.5, ^4J = 1.0, H^7), 8.14 (2H, d, ^3J = 8.0, $H^{3'}$), 8.01 (2H, dd, ^3J = 8.0, ^4J = 1.0, H^5), 7.97 (1H, t, ^3J = 8.0, $H^{4'}$), 7.74 (2H, dd, ^3J = 8.0, ^3J = 7.0, H^6), 7.61 (2H, dd, ^3J = 7.5, ^3J = 4.0, H^3).

4-Methoxy-2,6-di(8-quinolyl)pyridine L^2. A mixture of 4-methoxy-2,6-dibromopyridine (103 mg, 0.354 mmol), quinoline-8-boronic acid (202 mg, 1.17 mmol), $Pd(dba)_2$ (9 mg, 0.016 mmol) and K_3PO_4 (1.12 g, 5.27 mmol) in toluene (5 mL) was degassed by five freeze−pump−thaw cycles. 2-Dicyclohexylphosphino-2′,6′-dimethoxybiphenyl, "SPhos" (12 mg, 0.029 mmol) was added under a flow of nitrogen and the mixture stirred at 100 °C for 18 h. After cooling to room temperature, the mixture was filtered, the residue washed with dichloromethane, and the solvent evaporated from the combined filtrate under reduced pressure. Successive washing of the brown oily residue with small portions of diethyl ether led to the product as an off-white solid. ^1H NMR (500 MHz, $CDCl_3$) δ = 9.01 (2H, dd, ^3J = 4.0, ^4J = 1.5, H^2), 8.25 (2H, dd, ^3J = 7.5, H^7), 8.23 (2H, dd, ^3J = 6.5, ^4J = 1.5, H^4), 7.87 (2H, dd, ^3J = 7.5, ^4J = 1.5, H^5), 7.68 (2H, s, $H^{3'}$), 7.67 (2H, dd, ^3J = 7.5, 7.5, H^6), 7.45 (2H, dd, ^{3}J = 6.5, ^4J = 4.0, H^3), 3.98 (3H, s, OCH_3). MS (ES^+) m/z = 364 $[M+H]^+$. HRMS (ES+) m/z = 364.1443 $[M+H]^+$; calcd for $C_{24}H_{18}N_3O$ = 364.1444.

2,6-Di(N-7-azaindolyl)pyridine, L^3. A mixture of 2,6-dibromopyridine (200 mg, 0.84 mmol), 7-azaindole (300 mg, 2.53 mmol), K_2CO_3 (709 mg, 5.07 mmol), *trans*-1,2-diaminocyclohexane (29 mg, 0.25 mmol), and CuI (8 mg, 0.042 mmol) in dioxane (3 mL) was degassed by three freeze−pump−thaw cycles. The mixture was then heated at reflux under a nitrogen atmosphere for 72 h. The solvent was evaporated to yield a brown residue, which was extracted into CH_2Cl_2 and washed with water. The organic layer was dried over $MgSO_4$, and the solvent evaporated under reduced pressure. The resulting solid was washed with acetonitrile to yield L^3 as an off-white solid (154 mg, 59%). ^1H NMR ($CDCl_3$, 500 MHz): δ = 8.83 (2H, d, ^3J = 8.0, $H^{3'}$), 8.69 (2H, d, ^3J = 4.0, H^6), 8.44 (2H, dd, ^3J = 4.5, ^4J = 1.5, H^2), 8.06 (1H, t, ^3J = 8.0, $H^{4'}$), 7.98 (2H, dd, ^3J = 8.0, ^4J = 1.5, H^4), 7.19 (2H, dd, ^3J = 8.0, ^3J = 4.5, H^3), 6.68 (2H, d, ^3J = 4.0, H^5). ^1H NMR (d_6-DMSO, 500 MHz): δ = 8.83 (2H, d, ^3J = 8.0, $H^{3'}$), 8.68 (2H, d, ^3J = 4.0, H^6), 8.44 (2H, dd, ^3J = 4.5, ^4J = 1.5, H^2), 8.22 (1H, t, ^3J = 8.0, $H^{4'}$), 8.13 (2H, dd, ^3J = 8.0, ^4J = 1.5, H^4), 7.30 (2H, dd, ^3J = 8.0, ^3J = 4.5, H^3), 6.82 (2H, d, ^3J = 4.0, H^5). ^{13}C NMR ($CDCl_3$): δ = 149.4 ($C^{2'}$), 147.9 (C^8), 143.5 (C^2), 141.1 ($C^{4'}$), 129.4 (C^4), 126.5 (C^6), 123.6 (C^9), 117.5 (C^3), 111.8 ($C^{3'}$), 103.0 (C^5). MS (ES+) m/z: 312, $[M+H^+]$. HRMS (ES+) m/z: 312.1242; calcd for $C_{19}H_{14}N_5$ = 312.1244. Anal. Calcd. for $C_{19}H_{13}N_5(1/4H_2O)$: C, 72.25; H, 4.31; N, 22.17%. Found: C, 72.50; H, 4.18; N, 22.39%. Mp = 215−216 °C.

1,3-Di(8-quinolyl)benzene HL^4. Benzene-1,3-diboronic acid (0.100 g, 0.603 mmol) and 8-bromoquinoline (0.25 g, 1.201 mmol) were suspended in a mixture of toluene (6 mL), ethanol (6 mL), and sodium carbonate solution (2M, 3 mL), and the reaction mixture was degassed by four freeze−pump−thaw cycles. $Pd(PPh_3)_4$ (0.030 g, 0.026 mmol) was added under a positive pressure of nitrogen, and the solution heated under nitrogen at reflux for 42 h. After cooling to room temperature, water (5 mL) was added, and the product extracted into dichloromethane (3 × 5 mL). The combined extracts were dried over anhydrous $MgSO_4$, filtered, and the solvent removed under reduced pressure to yield a translucent oily solid. Purification was carried out via column chromatography (silica, hexane/ethyl acetate, elution gradient from 100:0 to 70:30) to yield a colorless solid (0.15 g, 76%). R_f (silica) = 0.1 in hexane/diethyl ether 50:50. ^{1}H NMR (500 MHz, $CDCl_3$) δ = 8.97 (2H, dd, ^3J = 4.0, ^4J = 2.0, H^2), 8.21 (2H, dd, ^3J = 8.5, ^4J = 2.0, H^4), 7.97 (1H, t, ^4J = 1.5, H$^{1'}$), 7.86 (2H, dd, ^3J = 7.0, H^5), 7.83 (2H, dd, ^3J = 7.0, H^7), 7.78 (2H, dd, ^3J = 7.5, ^4J = 1.5, H$^{3'}$), 7.63, (3H, overlapping t and dd, H$^{4'}$ and H^6), 7.42 (2H, dd, ^3J = 8.5, ^3J = 4.0, H^3). ^{13}C NMR ($CDCl_3$) δ = 157.0, 150.5, 150.1, 146.3, 145.7, 141.1, 139.4, 136.5, 133.0, 130.8, 129.7, 127.8, 126.6, 121.7, 121.2. MS (ES$^+$) m/z = 332 [M]$^+$. Anal. Calcd for $C_{24}H_{16}N_2$ = C, 86.72; H, 4.85; N, 8.43%. Found C, 86.47; H, 4.93; N, 8.43%.

Platinum Complexes. [PtL^{1}Cl]Cl and [PtL^{1}Cl]PF$_6$. A mixture of 2,6-di(8-quinolyl)pyridine L^1 (51 mg, 0.15 mmol) and $Pt(DMSO)_2Cl_2$ (78 mg, 0.19 mmol) in methanol (1.5 mL) was degassed by three freeze−pump−thaw cycles and then heated at reflux under a nitrogen atmosphere for 72 h. The precipitate that formed was collected by centrifugation and washed with water, methanol, and diethyl ether (3 × 5 mL of each), and dried under vacuum to give [PtL^{1}Cl]Cl as a pale gray solid (40 mg, 44%). Conversion to the hexafluorophosphate salt was achieved by dissolution of the chloride salt in the mimium volume of DMSO and addition to a saturated aqueous solution of KPF_6. The resulting precipitate was washed successively with water, methanol, and diethyl ether (3 × 5 mL of each) and dried under vacuum to give [PtL^{1}Cl]PF$_6$. Data for the chloride salt: ^{1}H NMR (d_6-DMSO, 500 MHz) δ = 9.25 (2H, d, ^3J = 4.5, H^2), 9.01 (2H, d, ^3J = 7.5, H^4), 8.92 (2H, d, ^3J = 7.0, H^7), 8.53 (2H, d, ^3J = 7.5, H^5), 8.47 (1H, t, ^3J = 8.5, H$^{4'}$), 8.32 (2H, d, ^3J = 7.5, H$^{3'}$), 8.09 (2H, dd, ^3J = 7.5, 7.0, H^6), 7.81 (2H, dd, ^3J = 7.5, ^4J = 4.5, H^3). MS (ES$^+$) m/z = 564 [M$^+$]. HRMS (ES$^+$) m/z = 563.0606. Calcd for $C_{23}H_{15}N_3{}^{35}Cl^{195}Pt$ = 563.0597. Anal. Calcd for $C_{23}H_{15}N_3Cl_2Pt$ = C, 46.1; H, 2.5; N, 7.0%. Found C, 45.7; H, 2.7; N, 6.6%. Data for the hexafluorophosphate salt: ^{1}H NMR (d_6-acetone, 700 MHz) δ = 9.37 (2H, dd, ^3J = 5.0, ^4J = 1.5, H^2), 9.02 (2H, dd, ^3J = 7.5, ^4J = 1.5, H^4), 8.97 (2H, d, ^3J = 7.5, H^7), 8.57 (2H, d, ^3J = 7.5, H^5), 8.54 (1H, t, ^3J = 8.5, H$^{4'}$), 8.40 (2H, d, ^3J = 8.5, H$^{3'}$), 8.13 (2H, dd, ^3J = 7.5, ^3J = 7.5, H^6), 7.84 (2H, td, ^3J = 7.5, ^4J = 5.0, H^3). ^{13}C NMR (d_6-acetone) δ = 158.1 (C^2), 151.5 (q), 142.0 (q), 141.9 (C^4), 141.5 (C$^{3'}$), 133.9 (q),133.4 (C^7), 132.6 (C^5), 129.2 (q),129.2 (C^6), 127.8 (C$^{4'}$), 123.3 (C^3). MS (ES$^+$) m/z = 564 [M$^+$]. HRMS m/z = (ES$^+$) 563.0611. $C_{23}H_{15}N_3{}^{35}Cl^{195}Pt$ requires 563.0597.

[PtL^{2}Cl]Cl and [PtL^{2}Cl]PF$_6$. The complex [PtL^{2}Cl]Cl was prepared in a similar way to [PtL^{1}Cl]Cl above, from L^2 (20 mg, 0.055 mmol) and $Pt(DMSO)_2Cl_2$, giving the product as a pale gray solid (17 mg, 52%). Ion exchange with aqueous KPF_6 gave the hexafluorophosphate salt. Data for the chloride salt: ^{1}H NMR (d_6-DMSO, 700 MHz) δ = 9.30 (2H, dd, ^3J = 5.0, ^4J = 1.5, H^2), 8.97 (2H, dd, ^3J = 7.5, ^4J = 1.5, H^4), 8.93 (2H, d, ^3J = 7.0, H^5), 8.49 (2H, d, ^3J = 7.5, H^7), 8.04 (1H, dd, ^3J = 7.5, ^{3}J = 7.0, H^6), 7.80 (2H, s, H$^{3'}$), 7.77 (2H, dd, ^3J = 7.5, ^4J = 5.0, H^3), 4.00 (3H, s, OCH_3). MS (ES$^+$) m/z = 594 [M$^+$]. HRMS (ES$^+$) m/z = 593.0713. Calcd for $C_{24}H_{17}N_3{}^{35}ClO\,{}^{195}Pt$ = 593.0704. Anal. Calcd for $C_{24}H_{17}N_3Cl_2OPt$ = C, 45.8; H, 2.7; N, 6.7%. Found C, 45.2; H, 3.1; N, 6.3%.

[PtL^{3}Cl]Cl and [PtL^{3}Cl]PF$_6$. A mixture of L^3 (0.050 g, 0.16 mmol) and $Pt(DMSO)_2Cl_2$ (0.087 g, 0.19 mmol) in methanol (3 mL) was degassed by freeze−pump−thaw five times. The mixture was refluxed under nitrogen for 3 d. The off-white precipitate was separated from the solution by centrifugation and washed with methanol, ethanol, diethyl ether, and dichloromethane to leave the product (53 mg, 57%). Conversion to the PF_6^- salt was performed by dissolution in the minimum volume of DMSO and dropwise addition of the solution to aqueous KPF_6. Data for the chloride salt: ^{1}H NMR (d_6-DMSO, 500 MHz): δ = 8.73 (2H, d, ^3J = 6.0, H^2), 8.61 (2H, d, ^3J = 4.5, H^6), 8.53 (2H, d, ^3J = 7.5, H^4), 8.46 (1H, t, ^3J = 8.0, H$^{4'}$), 7.90 (2H, d, ^3J = 8.5, H$^{3'}$), 7.58 (2H, dd, ^3J = 7.5, ^3J = 6.0, H^3), 7.34 (2H, d, ^3J = 4.5, H^5). ^{13}C NMR (d_6-DMSO): δ = 146.7 (C^2), 145.7 (C$^{3'}$), 145.2 (C^8), 144.4 (C$^{2'}$), 135.4 (C^4), 130.5 (C^6), 125.3 (C^9), 121.0 (C^3), 115.7 (C$^{4'}$), 110.3 (C^5). HRMS (ES+) m/z: 540.04783 [M$^+$]; calcd for $C_{19}H_{13}N_5Cl^{194}Pt$ = 540.04759. Anal. Calcd for $C_{19}H_{13}N_5Cl_2Pt$ = C, 39.5; H, 2.3; N, 12.1%. Found C, 39.0; H, 2.5; N, 11.7%. Data for hexafluorophosphate salt: ^{1}H NMR (CD_3CN, 400 MHz): δ 8.66 (2H, d, ^3J = 6.0, H^2), 8.31 (2H, d ^3J = 7.5, H^4), 8.27 (1H, t, ^3J = 8.5, H$^{4'}$), 8.01 (2H, d, ^3J = 3.5, H^6), 7.58 (2H, d, ^3J = 8.5, H$^{3'}$), 7.38 (2H, dd, ^3J = 8.0, ^3J = 6.0, H^3), 7.12 (2H, d, ^3J = 4.0, H^5).

PtL^{4}Cl. Separate solutions of HL^4 (50 mg, 0.15 mmol) in acetonitrile (3 mL) and K_2PtCl_4 (70 mg, 0.19 mmol) in water (1 mL) were degassed by three freeze−pump−thaw cycles. The latter was added to the former by cannula under a nitrogen atmosphere, and the mixture heated at reflux for 64 h. After cooling, the precipitate formed was separated by centrifugation, washed successively with water, ethanol, and diethyl ether (3 × 5 mL of each), and dried under vacuum leading to the complex as a gray-green solid (12 mg, 14%). ^{1}H NMR (500 MHz, $CDCl_3$) δ_H = 9.76 (2H, d, ^3J = 5.0, $^3J(^{195}Pt)$ = 48, H^2), 8.41 (2H, d, ^3J = 7.5, H^4), 8.37 (2H, d, ^3J = 7.5, H^7), 7.86 (2H, d, ^3J = 7.5, H^5), 7.72 (2H, dd, ^3J = 7.5, ^3J = 7.5, H^6), 7.58 (2H, d, ^3J = 8.0, $^4J(^{195}Pt)$ = 20, H$^{3'}$), 7.36 (3H, overlapping m, H^3 and H$^{4'}$). HRMS (ES+) m/z: 560.0542 [M$^+$]; calcd for $C_{24}H_{15}N_2ClPt$ = 560.0552. Anal. Calcd for $C_{24}H_{15}N_2ClPt$ = C, 51.3; H, 2.7; N, 5.0%. Found C, 51.1; H, 2.8; N, 4.9%.

[PtL^{1}OMe]PF$_6$. A mixture of [PtL^{1}Cl]PF$_6$ (30 mg, 0.042 mmol) and KOH (30 mg, 0.53 mmol) in methanol (3 mL) was stirred at room temperature for 18 h. The solution was concentrated and then added to saturated aqueous KPF_6 solution, leading to a bright yellow precipitate, which was collected by centrifugation, washed several times with water, and dried under vacuum to give the product (16 mg, 67%). ^{1}H NMR (400 MHz, $CDCl_3$) δ = 9.09 (2H, dd, ^3J = 5.0, ^4J = 1.5, H^2), 8.74 (2H, dd, ^3J = 7.5, H^7), 8.67 (2H, dd, ^3J = 8.0, 1.5, H^4), 8.42 (1H, t, ^3J = 8.0, H$^{4'}$), 8.25 (2H, d, ^3J = 8.0, H$^{3'}$), 8.16 (2H, d, ^3J = 8.0, H^5), 8.01 (2H, dd, ^3J = 8.0, ^3J = 7.5, H^6), 7.71 (2H, dd, ^3J = 8.0, ^4J = 5.0, H^3), 2.82 (3H, s, CH_3). MS (ES$^+$) m/z = 559 [M$^+$]. HRMS (ES$^+$) m/z = 559.1102. Calcd for $C_{24}H_{18}N_3O^{195}Pt$ = 559.1094.

[PtL^1(C≡C-tfp)]PF$_6$. Ethynyl-3,5-bis(trifluoromethyl)benzene (250 μL, 1.41 mmol) and potassium hydroxide (30.0 mg, 0.53 mmol) in methanol (5 mL) were stirred at room temperature for 1 h. A solution of [PtL^{1}Cl]PF$_6$ (40.0 mg, 0.071 mmol) and copper(I) iodide (4.0 mg, 0.021 mmol) in methanol (5 mL) was added, and the solution stirred overnight. The yellow precipitate formed was collected by centrifuge and washed with methanol to yield a yellow solid (17 mg, 31%). ^{1}H NMR (700 MHz, d_6-acetone) δ = 9.86 (2H, dd, ^3J = 5.0, ^4J = 1.0, H^2), 9.07 (2H, dd, ^3J = 8.0, ^4J = 1.0, H^4), 9.00 (2H, dd ^3J = 7.5, ^4J = 1.0, H^5), 8.55−8.57 (3H, m, H$^{4'}$ and H^7), 8.47 (2H, ^3J = 7.5, H$^{3'}$), 8.13 (2H, dd, ^3J = 7.5, ^3J = 7.5, H^6), 7.88 (2H, dd, ^3J = 8.0, ^4J = 5.0, H^3), 7.80 (1H, s, H$^{4\text{-tfp}}$), 7.78 (2H, s, H$^{2\text{-tfp}}$). ^{13}C NMR (d_6-acetone) δ = 160.3, 151.2, 142.6, 142.3, 141.7, 134.7, 133.4, 132.8, 131.8, 131.4, 131.1, 129.8, 129.2, 127.6, 123.5, 119.2, 110.2, 99.5, 97.2. ^{19}F NMR (d_6-acetone) δ = −63.9 (6F, s, CF_3), −73.4

(6F, d, ^2J = 700, PF_6^-). MS (MALDI$^+$-TOF, DCTB matrix) m/z = 765.2 $[M]^+$.

Electrochemistry. Cyclic voltammetry was carried out using a μAutolab Type III potentiostat with computer control and data storage via GPES Manager software. Solutions of concentration 1 mM in CH_2Cl_2 were used, containing $[Bu_4N][BF_4]$ as the supporting inert electrolyte. A three-electrode assembly was employed, consisting of a platinum working electrode, platinum wire counter electrode, and platinum flag reference electrode. Solutions were purged for 5 min with solvent-saturated nitrogen gas with stirring, prior to measurements being taken without stirring. The voltammograms were referenced to the ferrocene-ferrocenium couple.

DFT Calculations. B3LYP density functional calculations were performed using the Gaussian03 software package. Double-ζ quality basis sets were employed for the ligands (6-31G) and the Ir ion (LANL2DZ). The inner core electrons of Ir were replaced with a relativistic effective core potential, leaving the outer core $[(5s)^2(5p)^6]$ electrons and the $(5d)^6$ valence electrons of Ir(III). The geometries were fully optimized without symmetry constraints.

Photophysical Measurements. Absorption spectra were measured on a Biotek Instruments XS spectrometer, using quartz cuvettes of 1 cm path length. Steady-state luminescence spectra were measured using a Jobin Yvon FluoroMax-2 spectrofluorimeter, fitted with a red-sensitive Hamamatsu R928 photomultiplier tube; the spectra shown are corrected for the wavelength dependence of the detector, and the quoted emission maxima refer to the values after correction. Samples for emission measurements were contained within quartz cuvettes of 1 cm path length modified with appropriate glassware to allow connection to a high-vacuum line. Degassing was achieved via a minimum of three freeze−pump−thaw cycles while connected to the vacuum manifold; final vapor pressure at 77 K was $< 5 \times 10^{-2}$ mbar, as monitored using a Pirani gauge. Luminescence quantum yields were determined using $[Ru(bpy)_3]Cl_2$ in degassed aqueous solution as the standard (ϕ = 0.042[41]); estimated uncertainty in Φ is ± 20% or better.

The luminescence lifetimes of the complexes were measured by time-correlated single-photon counting, following excitation at 374.0 nm with an EPL-375 pulsed-diode laser. The emitted light was detected at 90° using a Peltier-cooled R928 PMT after passage through a monochromator. The estimated uncertainty in the quoted lifetimes is ±10% or better. Lifetimes at 77 K in excess of 10 μs were measured by multichannel scaling following excitation with a μs-pulsed xenon lamp; an excitation wavelength of 374 nm (band-pass 5 nm) was selected with a monochromator. Bimolecular rate constants for quenching by molecular oxygen, k_Q, were determined from the lifetimes in degassed and air-equilibrated solution, taking the concentration of oxygen in CH_2Cl_2 at 0.21 atm O_2 to be 2.2 mmol dm^{-3}.[42]

Acknowledgment. We thank EPSRC and the University of Durham for financial support, Frontier Scientific for supplying key reagents, and Octavia Blackburn for preparing a sample of $[PtL^3Cl]^+$.

Supporting Information Available: Representative mass spectrum and additional ^{1}H NMR spectra; frontier orbital plots of the complexes, including HOMO−1 and LUMO+1, obtained by DFT calculations; absorption and emission spectra of complexes not shown in the main text; emission spectra of ligands at 77 K; influence of solvent on absorption and emission spectra. This material is available free of charge via the Internet at http://pubs.acs.org.

(41) Van Houten, J.; Watts, R. J. *J. Am. Chem. Soc.* **1976**, *98*, 4853.
(42) Murov, S. L.; Carmichael, I.; Hug, G. L. *Handbook of Photochemistry*, 2nd ed.; Marcel Dekker: New York, 1993.